MtNIP5;1, A Novel Medicago Truncatula Boron Diffusion Facilitator Induced Under Deficiency

Sara Granado-Rodríguez
Universidad Autonoma de Madrid
Luis Bolaños
Universidad Autonoma de Madrid
Maria Reguera (maria.reguera@uam.es)
Universidad Autonoma de Madrid https://orcid.org/0000-0001-5939-8576

Research article

Keywords: Boron deficiency, Medicago truncatula, aquaporins, MtNIP5;1, boron transport, legumes

Posted Date: June 30th, 2020

DOI: https://doi.org/10.21203/rs.3.rs-35531/v1

Version of Record: A version of this preprint was published on December 9th, 2020. See the published version at https://doi.org/10.1186/s12870-020-02750-4.

Abstract

Background: Boron (B) uptake in plants implies a passive diffusion through membranes under optimal conditions. Under deficiency or toxicity, the participation of two distinct protein families (the aquaporin family Major intrinsic proteins (MIPs) and the Boron transporter family BOR) is required to minimize detrimental effects caused by B stress that ends up inhibiting growth and altering development. Legumes comprise important crops that offer major agronomic benefits including the capacity of establishing symbiosis with rhizobia fixing atmospheric N_2 and for being important food protein sources. It is well proven their susceptibility to B stress leading to important yield penalties. However, little is known about the transport mechanisms responsible for B uptake and distribution in legumes, especially under deficiency.

Results: A novel legume B transporter involved in B uptake under deficiency, the *Medicago truncatula* homologous protein MtNIP5;1 (Medtr1g097840) to the *Arabidopsis thaliana* AtNIP5;1 (sharing 73,7% amino acid identity) was identified. Further analyses revealed that this *M. truncatula* aquaporin expression was boron-regulated in roots, being induced under deficiency and repressed under toxicity. It localizes at the plasma membrane of root epidermal cells and in nodules, where B plays pivotal roles in symbiosis. Furthermore, a partial complementation of the *nip5;1* Arabidopsis mutant phenotype under B deficiency supports a functional role of MtNIP5;1 as a B transporter of in this legume model plant.

Conclusions: The results here presented support a functional role of MtNIP5;1 uptaking B under deficiency providing new insights into this micronutrient transport mechanisms in legume species.

Background

Boron (B) is an essential micronutrient for plants as it plays an structural role in plant cell walls, crosslinking two pectin polysaccharides rhamnogalacturonan-II (1, 2). When B concentrations are below optimum, B-deficiency symptoms appear and include the inhibition of root elongation, a reduced leaf expansion and fertility, resulting in substantial agronomical loses around the world (3–5).

In soils, B is mainly found as uncharged boric acid [$B(OH)_3$] (Ka = 5.80 × 10–10 at 25 °C (pKa = 9.24)) (6). At optimal concentrations, B enters the plant through passive diffusion. However, under deficiency, B is transported into and within the plant by the coordinated action of proteins that belong to two protein families: the aquaporin family Major intrinsic proteins (MIPs) and the Boron transporter family BOR (7–10).

MIPs are a superfamily of aquaporins made up of several subfamilies, including the nodulin-26-like intrinsic proteins (NIPs) (11). NIPs are permeable channels to small solutes including [$B(OH)_3$] (12–16). The best characterized NIP protein characterized as a B facilitator transporter is the *Arabidopsis thaliana* NOD26-like intrinsic protein 5;1 (AtNIP5;1), a cell membrane channel permeable to water, urea and

$[B(OH)_3]$ (17). It is found in epidermal cells of roots and its transcripts are up-regulated under low B conditions increasing B permeability and maximizing B uptake from B-deficient soils (15).

BOR is a family of boric acid and borate exporters, with seven members identified in *A. thaliana* (AtBOR1-7) (18, 19). AtBOR1 accumulates under low-B conditions in the root stele, and performs xylem loading of $[B(OH)_3]$ from where B is distributed to the rest of the plant (7, 18). It has been proven that the coordinated action of AtNIPs and AtBOR1s is essential to ensure a proper B distribution within the plant, specially under low-B conditions, what is required for a proper plant growth and development (20).

Among crops of agronomical interest are members of the legume family (*Leguminosae* or *Fabaceae*), such as alfalfa, pea or soybean (21), which have the ability to interact symbiotically with N_2-fixing Rhizobia triggering the formation of root nodules where biological nitrogen fixation takes place (22–24). Every step of the establishment of Legume-rhizobia symbioses is severely altered by B deficiency (Bolaños et al., 1996, 2001; Redondo-Nieto et al., 2007; Reguera et al 2009; 2010; 2019).

On the other hand, developing more efficient nitrogen-fixing associations is of high importance given the pollution problems associated with the excessive use of chemical fertilizers (25, 26), and requires a better understanding of which are the factors, including nutrient transport, determining the success of the process (27–29).

Despite being a key element for plant growth and development and for the establishment and manteinance of the legume-rhizobia symbiosis, B transport has been barely studied in legumes, and only one B transporter that functions under toxic B concentrations has been characterized in the model plant *Medicago truncatula* Gaertn so far (30). In the present study, using a candidate gene approach combined with a phenotypic analysis and a heterologous complementation assay, we characterize *MtNIP5;1* as a novel B transporter of *M. truncatula*, homologous to AtNIP5;1, that functions under low boron conditions. The results presented here will allow gaining further knowledge regarding B nutrition in leguminous plants.

Results

Boron stress causes developmental and growth defects in Medicago truncatula

In order to study *M. truncatula* response to B availability, a growth assay was carried out applying a B gradient. The plant phenotype and nitrogenase activity (for those plants growing under symbiotic conditions) were analyzed.

Plants growing under B deficiency showed chlorosis and the inhibition of leaf expansion and root growth. Generally, these symptoms were more evident in nodulated plants than in those fertilized with N (Fig. 1). Fewer and smaller nodules appeared in these plants compared to those growing under control conditions

(Fig. 1). On the other hand, plants growing under B toxicity showed a comparable growth inhibition under symbiotic and non-symbiotic conditions. Generally, nodules of plants growing under B toxicity presented similar sizes although it was noticeable a significant number of nodules with a smaller size.

Biomass data supported most of these observations (Fig. 1A-C). Biomass reduction (of approximately 60%) was observed in roots of both N-fertilized and nodulated plants growing under B deficiency (Fig. 1B). A reduced nodule biomass was also found under deficiency (Fig. 1C). Under toxicity, plants showed a decreased in shoot and root biomass under symbiotic and non-symbiotic conditions (Fig. 1B). Nonetheless, nodules did not show an altered biomass under high B levels (Fig. 1C).

Nitrogenase activity was determined and expressed per plant (Fig. 1D) or relative to nodule number or nodule weight (Additional file 2), giving all similar results. Nodules of both B-deficiency and B-toxicity growing plants showed a significant reduction of nitrogenase activity. These results were consistent with the observed nodule defects observed under B deficiency. Interestingly, despite no significant differences were observed under B toxicity in nodule biomass, N fixation was severely affected under these conditions.

Identification of AtNIP5;1 homologs in M. truncatula

The *A. thaliana* nodulin 26-like intrinsic protein *NIP5;1*, encoding an aquaporin that belongs to the Major Intrinsic Protein (MIP) family, was the first aquaporin in plants involved in boron transport in plants (15). Sequence comparison of the encoded protein *AtNIP5;1* (*AT2G47160*), showed that *Medtr1g097840* (named MtNIP5;1) is the closest homolog to the *A. thaliana* B transporter in *M. truncatula*, showing 73,7% sequence identity (Fig. 2A).

Aiming to further characterize the MtNIP5;1 protein, a 3D protein structure prediction was performed using bioinformatics. The predicted tertiary structure indicated that the encoded protein would be transmembranous, presenting six membrane-spanning helices, connected through loops, and two short helices connected via conserved NPA-motifs (Asn-Pro-Ala) together forming the seventh transmembrane helix (Fig. 2B). The distribution of these seven helices would constitute a pore, a characteristic feature of aquaporin proteins (31). Besides, the protein charge layout indicated the location of positive charged residues in the external part of the pore, leaving the negative charges in the inside. On the other hand, the comparisons with other MIP proteins (such as the AtTIP2;1 (AT3G16240), whose selectivity filter is composed by H63, H131, I185, G194 and R200) revealed that MtNIP5;1 contains 5 amino acids (F58, N129, H180, G190 and R197) that would conform the selectivity filter of this aquaporin.

MtNIP5;1 expression is induced under B deficiency

In order to evaluate possible changes in the expression patterns of *MtNIP5;1* under a B gradient a qPCR assay was performed in three different tissues (roots, nodules and aerial parts of nodulated and non-nodulated plants). *MtNIP5;1* expression was induced under B deficiency in both shoots and roots, although it was more pronounced in the latter. Besides, the expression was repressed in roots under B toxicity compared to control conditions. Nodules presented lower transcripts levels compared to shoots

and roots and the induction did not change significantly among the three B conditions tested (Fig. 3A). *In silico* analysis based on the symbimics database (https://iant.toulouse.inra.fr/symbimics/) or the Medicago Gene Expression Atlas (https://mtgea.noble.org/v3/, ID Mtr.34598.1.S1_at) support these results showing a much higher expression in roots compared to other plant organs (including nodules or the shoot/aerial part) (Additional file 3).

Going furhter, the tissue expression of this gene was evaluated by fusing the β-glucuronidase gene (*gus*) to the *MtNIP5;1* promoter. *M. truncatula* seedlings were transformed with a construct containing the 2 kb region upstream of *MtNIP5;1* fused to *gus*. The blue GUS staining was detected in roots and nodules of control and B-deficient plants 4 weeks postinoculation (Fig. 3B). As indicated by qPCR, *MtNIP5;1* was highly expressed in roots, especially under B deficiency. More specifically, the activity was located at the root vasculature. Nodules also presented GUS activity located in he vasculature zone, with a more intense signal under B deficiency (Fig. 3B)

MtNIP5;1 localizes at the plasma membrane in the epidermis of roots and in epidermical and cortical cells of nodules

Transient transformation of *Nicotiana benthamiana* leaves was performed aiming to analyze the subcellular location of MtNIP5;1. *Agrobacterium tumefaciens* containing either *p35S::MtNIP5;1-GFP* or *p35S::AtPIP2A-CFP* constructs were co-infiltrated as described in the Methods section. An overlapping signal was observed between MtNIP5;1 fused to the GFP fluorophore and the plasma membrane marker indicating that MtNIP5;1 is located at the plasma membrane (Fig. 4). Controls in which no florophores were used, showed no signal in the measured channels (Additional file 4). Also, a positive agroinfiltration control using p35S:: GFP was used (Suppl. Figure 3).

The chimeric MtNIP5;1-HA protein was used in the immunohistochemical studies. *M. truncatula* plants were transformed with the genomic region of *MtNIP5;1* fused in-frame with three haemagglutinin (HA) epitopes in the C-terminus (MtNIP5;1-HA), using the same promoter region as the one used for the GUS assay. MtNIP5;1-HA was detected (DsRed channel) with a mouse anti-HA antibody and an Alexa594-conjugated anti-mouse secondary antibody. Images showed protein localization at the epidermal cells of roots (Fig. 5A), under both B conditions. Besides, in nodules, the protein signal appeared in some infected nodule cells and nodule cortex (Fig. 5B). Results using, as an alternative chimera, MtNIP5;1-GFP, gave similar results as the HA fusion, supporting protein localization results (Additional file 5). On the other hand, MtNIP5;1-HA (nor MtNIP5;1-GFP) signal distribution was not consistent with the tissue specific expression observed in the GUS staining assays where an intense signal appeared located exclusively at the vasculature of roots and nodules (Fig. 5). Controls in which no Alexa 594-conjugated antibody was used showed no signal in the measured channels (Fig. 5).

Partial complementation of nip5;1 A. thaliana mutant supports a role of MtNIP5;1 as a B transporter

Aiming to characterize functionally this putative B transporter, a heterologous expression system in *A. thaliana* was used. Thus, the *A. thaliana nip5;1–1* mutant (15) was transformed with the *p35S:: MtNIP5;1-*

GFP construct and two independent homozygous single copy lines were obtained (*p35S:: MtNIP5;1 -GFP* 1 and *p35S:: MtNIP5;1 -GFP* 2). These lines were used to test MtNIP5;1 capability to complement the mutant phenotype. WT, *nip5;1–1* and *nip5;1–1* mutant lines overexpressing MtNIP5;1 were grown under two B conditions, control (100 μM $B[OH]_3$) and deficiency (0,03 μM $B[OH]_3$), and the primary root length of these seedlings was quantified over the time (Additional file 6).

The effect of reduced B availability on primary root length was already noticeable at 3 DPG, moment in which *nip5;1–1* roots started showing a significantly lower length compared to the Wt or the two mutant lines expressing *MtNIP5;1*. In fact, at the end of the experiment (10 dpg), both mutant lines overexpressing *MtNIP5;1* showed approximately double lenght of the mutant primary root growing under B deficient conditions and about half of the Wt root size, confirming a partial complementation of the mutation by overexpression of *MtNIP5;1* (Fig. 6).

Discussion

Boron is an essential micronutrient for plants that, below optimal concentrations, limits growth and development affecting plant productivity worldwide (32, 33). Legumes comprise important plant species widely used as grain (i.e. beans) and forage (i.e. alfalfa) crops that can interact symbiotically with soil bacteria (rhizobia) fixing atmospheric N_2 (34). They are especially sensitive to B stress (deficiency or toxicity) under non-symbiotic conditions (35, 36) and symbiotic conditions (37, 38). Particularly B deficiency has proven impact on the establishment and maintenance of the symbiotic interaction with rhizobia (37, 39, 40). Thus, under the context of food security, sustainable agriculture and climate change, the interest of understating B transport and B stress tolerance in legumes, particularly under symbiotic conditions, has been increasingly higher, aiming to minimize the impact of this nutrient stress on yields (41, 42). Thus, this work, by using the model legume plant *M. truncatula*, aimed to further understand B transport in legumes, considering that no B transporter involved in B transport under deficient conditions has been characterized till date in this agronomically important plant family.

Plant aquaporins are transmembrane channels implicated in the facilitated transport of water and other small non-charged solutes such as boric acid (43) Together with the energy-dependent high-affinity B transport system constituted by the BOR family, different members of the Major Intrinsic Protein (MIP) family possess a role transporting (and therefore, distributing) B in plants (15, 44). The nodulin 26 (NOD26) protein NIP5;1 was the first described aquaporin implicated in the uptake of B from the soil into the roots acting coordinately with AtBOR1 (identified and characterized few years earlier) to ensure the uptake and correct distribution of B under deficient conditions (15, 45). From there, the use of homology-based analysis has allowed the identification of many B transporters in different plant species (including rice, barley or *M. truncatula*), however, most of these are functionally related to an increased tolerance to high B (i.e. MtNIP3, (30)) .

Many different MIP family members, including those that belong to the Tonoplast membrane Intrinsic Proteins (TIP) subfamily (such as AtTIP5;1 (46)) or to the Plasma membrane Intrinsic Proteins (PIP)

subfamily (such as the barley Hv-PIP1;3 and Hv-PIP1(12), the maize ZmPIP1 (47) or the rice OsPIP2;4, OsPIP2;7, OsPIP1;3 and OsPIP2;6 members (48)), have been found to be involved in the transport of B in plants. In *M. truncatula*, a close relative to the forage legume alfalfa widely used as a model plant for genetic and genomic studies(49), MtNIP3 was identified as an homologous protein to AtNIP6;1 (sharing 75% of amino acid sequence similarity). MtNIP3 physiological role was related to conferring a high B tolerance as showed higher leaf expression levels in B tolerant cultivars what correlated positively with lower B ^{concentrations} in leaves (30).

In the present study, we search for homologues to AtNIP5;1 in *M. truncatula* aiming to identify putative B transporters involved in B transport under B deficiency. The analysis yielded MtNIP5;1 protein as the most promising candidate that may function as AtNIP5;1 due to the amino acid sequence similarity (sharing 73,7% amino acid identity, Fig. 2A). This protein was previously pointed as a putative B transporter homolog to AtNIP5;1 by (30) although no analysis were carried to further prove its role nor understand its function as this work focused on studying the role of another *M. truncatula* NIP protein, MtNIP3 (Medtr4g006730.1), as mentioned earlier, a B transporter functioning under B toxicity. This and our results, support distinct roles of NIP proteins in B transport, being involved in toxicity and deficiency responses (14, 15). In here, qPCR analysis and GUS expression assays showed that B deficiency induces *MtNIP5;1* expression mainly in roots, but also in shoots. Furthermore, B toxicity is able to repress this gene expression specifically in roots supporting a possible role of this *M. truncatula* NIP protein uptaking B and being regulated by B conditions.

Interestingly, at the end of the 5' untranslated region (5'UTR) of *MtNIP5;1*, right before the ATG starting codon, an accumulation of 8 thymine nucleotides and 20 adenine nucleotides appeared (nucleotide sequence of this area shown in Additional file 7A). This sequence is presented in a distinctive zone and due to the characteristic nucleotide sequence, it may play pivotal roles in *MtNIP5;1* expression regulation under different B conditions as it happens with the 5' UTR of AtNIP5;1. In AtNIP5;1, the 5'UTR has been shown to be involved in NIP5;1 transcript accumulation in response to B conditions (50). This raises interesting questions regarding this *M. truncatula* gene regulation under B toxicity, conditions that were correlated with lower transcripts levels (Fig. 3A). Noteworthy, although both *A. thaliana* and *M. truncatula* genes share quite high 5´UTR sequence similarity (Additional file 7B), the characteristic nucleotide composition presented at the end of the 5´UTR region in the *M. truncatula* gene does not appear in AtNIP5;1 indicating that may be a particular feature of the *M. truncatula* gene.

Going further in the analysis, MtNIP5;1 3D structure was predicted based on the crystallized structure of AtTIP2;1 (AT3G16240), an aquaporin permeable to ammonia that belongs to the MIP superfamily, as it does AtNIP5;1 (51). From this analysis, it was inferred that MtNIP5;1 is a transmembrane protein according to its predicted structure, similar to AtTIP2;1 and conserved among aquaporins (presenting seven helices with neutral charge distribution) ((51, 52), Fig. 2B). Also, AtNIP5;1 was described as a transmembrane protein located in the plasma membrane (17). Besides, the presence of NPA motifs in MtNIP5;1 are also a conserved feature among aquaporins, whose function is to facilitate the exit of protons when solutes pass through the channel (51). Furthermore, aquaporins have a selectivity filter

made up of five amino acids. These are different between AtTIP2;1 and MtNIP5;1, pointing to an evolutionary differentiation of their functions so that MtNIP5;1 could be permeable to other molecules, such as boric acid.

In *A. thaliana*, AtNIP5;1 localizes at the plasma membrane of root epidermal cells functioning as a boric acid channel responsible for B uptake under B limited conditions (17). In here, protein localization showed similar patterns. MtNIP5;1 appeared localized at the plasma membrane and at the root epidermal cells, what fits well with a role of this facilitator protein ensuring B incorporation under B deficiency. Furthermore, expressing *MtNIP5;1* under the control of CaMV 35S promoter complemented partially root growth defects shown by *nip5;1* under B deficiency (0,03 µM B[OH3]) (Fig. 6). These results suggest, on one hand, that *MtNIP5;1*-GFP is functional *in planta* and on the other, that *MtNIP5;1* shares functional similarities with AtNIP5;1.

Furthermore, several reports have shown the symbiosis reliance on B (37, 53–56) although no B transporter was characterized in this organ until now. Regarding this point, it was initially hypothesized that MtNIP5;1 could play a distinctive role in nodules transporting B under deficiency. However, and despite observing that MtNIP5;1 localizes to this organ (Fig. 5B) and therefore, being the first nodule B transporter identified in nodules, the lack of expression induction under deficiency does not support a unique role of this transporter in B uptake under deficiency in nodules. Nonetheless it should not be discarded a helper role of this aquaporin in B uptake under B limiting conditions in nodules, based on its expression and localization patterns.

Conclusions

Overall, the studies here performed aimed at characterizing putative B transporters of *M. truncatula* belonging to the aquaporin NIP subfamily, functioning under deficiency. A homology-based analysis pointed to *MtNIP5;1* as the most promising candidate to function as AtNIP5;1 in this legume model plant. The induced expression under B deficiency and the repression under B toxic levels, together with this protein localization patters and the partial complementation of *nip5;1* mutant, support a role of MtNIP5;1 functioning as a B transporter under B deficiency. These results might help better understanding B transport in legumes what could help developing tolerant cultivars better adapted to B deficient soils. In line with this, it would be interesting to investigate further if legume tolerant varieties present higher expression of this *MtNIP5;1* (or homologous candidates), as has been done with other aquaporins in *M. truncatula* or barley, in which it has been linked tolerance to B toxicity with gene function.

Methods

Plant growth conditions

Seeds of *Medicago truncatula* ecotype R108, obtained from Dr. González-Guerrero´s Laboratory (CBGP-UPM/INIA, Spain), were scarified with sulfuric acid (H_2SO_4), sterilized with bleach before they were

germinated in 0,8% agar plates and placed in the dark at 4 °C for 48 h, following the steps described by (Tejada-Jiménez et al., 2015). After stratification, plates were moved to a growth chamber at 22 °C for 24 h with a 16h:8 h light:dark cycle. Seedlings used for phenotypic or RT-qPCR analyses were transferred to pots using perlite as a substrate and grown in the greenhouse with a long-day photoperiod (16h:8 h light:dark cycle at 18–25 °C). Greenhouse plants were irrigated every two days with Jenner's solution or water, alternatively (57). Jenner's solution was supplemented or not with B (to achieve control or B deficient conditions) and N (to achieve symbiotic or non-symbiotic conditions))

Nicotiana benthamiana Domin plants, obtained from Dr. González-Guerrero´s Laboratory (CBGP-UPM/INIA, Spain), were pre-germinated in peat for 10–15 days at 20–22 °C with a 16h:8 h photoperiod. They were then transplanted to peat:vermiculite 3:1 and grown for 3–4 weeks in a greenhouse at 18–25 °C and long-day photoperiod.

Arabidopsis thaliana ecotype Col-0 and *nip5;1–1* mutant seeds (58), obtained from Dr. Miwa Laboratory (Hokkaido University, Japan), were sterilized first in ethanol 70% and then in bleach 50% with a droplet of Tween-20. After rinsing well the seeds with H_2O_d, they were kept overnight in the dark at 4 °C and then germinated in plates with half strength MS media (59). For segregation experiments, seedlings were transplanted to peat:perlite 3:1 and grown in a growth chamber at 23 °C with long-day photoperiod.

Phenotypic analysis

In order to study B-availability effects on plant growth, inoculated and non-inoculated *M. truncatula* plants were irrigated with different concentrations of H_3BO_3. Control treated plants were irrigated with 0,1 mM H_3BO_3, toxicity conditions were achieved irrigating plant with a final H_3BO_3 concentrations of 1 mM and no H_3BO_3 was applied for deficiency conditions. All irrigation media was treated with Amberlite® IRA743 to eliminate B traces.

Plants grown under symbiotic conditions were inoculated with *Sinorhizobium meliloti* FSM-MA strain (60) without receiving any external input of N (-N). Non-inoculated plants were supplemented with 20 mM NH_4NO_3 (+ N).

Plant tissue was collected 5 weeks after the transplant (4 weeks after inoculation) for biomass measurements, nitrogenase activity and RT-qPCR assays.

Biomass, as fresh weight, was determined immediately after plant harvesting. Biomass, as dry weight, was determined after drying the plant tissue at 60 °C for 72 h.

Nitrogenase activity was measured using the acetylene reduction assay as described by Hardy *et al.* (1968). Briefly, roots of nodulated plants were placed in 30 ml vials where 3 ml of air were replaced with 3 ml of acetylene. After 30 minutes, 4 replicates of 0,5 ml each were extracted and their ethylene content was measured using a gas chromatograph Shimadzu GC-2014 (Japan). A dilution of ethylene and acetylene 0,413 mg/l was used as standard. At the end, nodules were counted and weighed.

Gene candidate identification

To identify *AtNIP5;1* homologous genes that putatively encode B facililator trasnporters in *M. truncatula*, the *AtNIP5;1* (*At4g10380*) sequence was obtained from the TAIR database (https://www.arabidopsis.org/) and BLAST in the *M. truncatula* genome using the Phytozome database (https://phytozome.jgi.doe.gov/pz/portal.html).

Gene expression analysis by RT-qPCR

Gene expression studies were carried out by real-time RT-PCR (Applied Biosystems®) in order to analyze transcript levels of candidate genes. ARN Extraction was carried out using the RNeasy Mini Kit (Qiagen). cDNA was obtained from 500 ng of DNA-free RNA using PrimeScript™ (Takara Bio Inc., Japan). Primers used are indicated in Additional file 1. RNA levels were normalized by using the *ubiquitin carboxy-terminal hydrolase* gene as internal standard for *M. truncatula* expression patterns (62).

M. truncatula transformation

The *Agrobacterium rhizogenes* ARqua1 strain containing the vector was used to transform *M. truncatula* seedlings after 18 h germination in a growth chamber at 22 °C. Transformation experiments were performed following the protocols described by Boisson-Dernier *et al.* (2001). Transformed seedlings were later transferred to Farhaeus media plates supplemented with kanamycin (50 µg/ml) as selection marker (64). After three weeks, plants were transplanted to sterile perlite pots that were placed in the greenhouse at 18–25 °C and long-day photoperiod.

GUS staining

The *MtNIP5;1* promoter:: β-glucuronidase (GUS) construct was generated using the Gateway System (Life Technologies, Carlsbad, USA). The promoter fragment of the candidate gene (2.022 kb upstream of the *MtNIP5;1* start codon, $P_{-1174\ UT848}$) was amplified using the primers indicated in Additional file 1, cloned in the pDONOR27 vector (Invitrogen) and transferred to the pGWB3 plasmid (65).

Gus activity assay was performed in plants 4 weeks after inoculation following the protocol described by (66) with minor modifications. Roots and nodules sections (100 µm) were incubated in a GUS buffer (0,69% PO_4H_2Na, 0,5 M EDTA pH 8, 0, 30% sarkosyl, 40 µl triton X-100 AND H_2O) supplemented with X-Gluc (0,1 mg/ml) for 12–16 h at 28 °C in the dark, and then distained with bleach 50% and rinsed five times in H_2O. Afterwards, sections were observed with a Leica DM IRB microscope.

Immunohistochemistry and confocal microscopy

MtNIP5;1 gene and its native promoter (2 kb upstream of the start codon) were amplified with the primers indicated in Additional file 1 and cloned into the plasmid pGWB13 that fuses three C-terminal hemagglutinin (HA) tags in-frame or into the pGWB4 plasmid that fuses the GFP (green fluorescent protein) tag (65), using the Gateway system (Life Technologies, Carlsbad, USA).

Transformed plants were inoculated with *S. meliloti* 2011. Roots and nodules were fixed overnight in a 4% paraformaldehyde, 2.5% sucrose and PBS buffer at 4 °C. After several washes in PBS, the tissue was embedded in 6% agarose and 100 µm sections were prepared in a Vibratome 1000 plus. Sections were dehydrated using methanol series (30, 50, 70, 100% in PBS) for 5 min and then rehydrated. The immunostaining was started permeabilizing plant cell walls with 4% cellulase in PBS for 1 h at RT and with 0.1% Tween 20 in PBS for 15 min. Sections were blocked with 5% bovine serum albumin (BSA) in PBS before their incubation with anti-HA mouse monoclonal antibody (Sigma) for 2 hours at room temperature. After several washes, sections were incubated for 1 h with Alexa594-conjugated anti-mouse rabbit monoclonal antibody (Sigma). Images were acquired using a confocal laser-scanning microscope (Leica SP8) at 488 nm and 561 nm for GFP and Alexa 594, respectively.

N. benthamiana transient expression assay

The *MtNIP5;1* gene was amplified using the primers indicated in Additional file 1, and then cloned into the pGWB5 plasmid, which fuses the cauliflower mosaic virus 35S RNA (CaMV 35S) promoter and the GFP tag C-terminally (65). *A. tumefaciens* C58C1 (67) was transformed with either *p35S::MtNIP5;1-GFP* or the the construct *p35S::AtPIP2A*- cyan fluorescent protein (CFP) (68) together with the silencing suppressor p19 of the Tomato bushy stunt virus (69). *N. benthamiana* 3 weeks-old leaves were then infiltrated following the protocol described by Sparkes *et al.* (2006). Images were taken 48 h after agroinfiltration with a confocal microscope (Leica SP8).

Bioinformatic analysis

The aminoacidic sequence of the gene candidate was obtained from the database UniProt (http://www.uniprot.org/). Protein 3D models were predicted using I-TASSER (https://zhanglab.ccmb.med.umich.edu/I- TASSER/) and were edited with the software PyMol.

A thaliana mutant complementation assay

A. tumefaciens strains containing the construct *p35S::MtNIP5;1-GFP* were used to transform the *nip5;1–1 A. thaliana* mutant (58) using the floral dipping transformation method as described by (71). Homozygous lines containing the construct of interest were selected by kanamycin selection and PCR analysis, using the primers included in Additional file 1. Seeds of *A. thaliana* Col-0 (wildtype, WT), the mutant *nip5;1–1*, and two homozygous independent lines incorporating the construct *p35S::MtNIP5;1-GFP* were grown vertically in plates of ½ MS medium with two B treatments: control (100 µM $B[OH]_3$) and deficiency (0,03 µM $B[OH]_3$). Primary root length was then measured at 3, 5, 7 and 10 days post germination, from the root tip to the hypocotyl boundary, using the online available softwre ImageJ (http://rsbweb.nih.gov/ij/).

Statistical Analysis

One-way analysis of variance (ANOVA) followed by a Tukey HSD *post-hoc* test were applied to perform multiple comparisons at a probability level of 5% ($p < 0.05$). The SPSS Statistics 17.0 (SPSS Inc.) package was used for the statistical analyses.

Abbreviations

B Boron

MIP Major intrinsic protein family

BOR Borate transporter family

NIP Nodulin-26-like intrinsic protein family

Declarations

Acknowledgments

The authors greatly thank Dr. Manuel Gonzalez-Guerrero for his support helping to conceive and plan the experiments. Also, we thank Dr. Toru Fujiwara (University of Tokyo, Japan), Dr. Junpei Takano (Osaka Prefecture University, Japan) and Dr. Kyoko Miwa (Hokkaido University, Japan) for providing the Arabidopsis *nip5;1-1* mutant seeds used in this study. The authors declare no conflict of interest.

Authors contribution statement

M.R conceived and planned the experiments. M.R. carried out most part of the experiments. S.G.R carried out the mutant complementation assays. M.R and S.G.R contributed to the interpretation of the results. M.R. took the lead in writing the manuscript with L.B contribution. All authors provided critical feedback and helped shape the research, analysis and manuscript.

Funding

The author(s) received no specific funding for this work.

Author information

Affiliations:

Departamento de Biología, Universidad Autónoma de Madrid, c/Darwin 2, Campus de Cantoblanco, 28049, Madrid, Spain.

Declarations

Availability of data and materials

All data generated or analyzed during this study are included in this published article (and its additional files).

Ethics declarations

Ethics approval and consent to participate

Not applicable.

Consent for publication

Not applicable.

Competing interests

The authors declare that they have no competing interests.

References

1. Warington K. The Effect of Boric Acid and Borax on the Broad Bean and certain other Plants [Internet]. Vol. 37, Annals of Botany. Oxford University Press; 1923 [cited 2020 Jun 5]. p. 629–72. Available from: https://www.jstor.org/stable/43236455.
2. O'Neill MA, Eberhard S, Albersheim P, Darvill AG. Requirement of Borate Cross-Linking of Cell Wall Rhamnogalacturonan II for Arabidopsis Growth. Science (80-). 2001;294(5543).
3. Koshiba T, Kobayashi M, Matoh T. Boron deficiency: How does the defect in cell wall damage the cells? Plant Signal Behav. 2009 Jun;4(6):557–8.
4. http://doi.wiley.com/10.1055/s-2002-25740
   Brown PH, Bellaloui N, Wimmer MA, Bassil ES, Ruiz J, Hu H, et al. Boron in Plant Biology. Plant Biol [Internet]. 2002 Mar [cited 2016 Oct 28];4(2):205–23. Available from: http://doi.wiley.com/10.1055/s-2002-25740.
5. Shireen F, Nawaz MA, Chen C, Zhang Q, Zheng Z, Sohail H, et al. Boron: Functions and approaches to enhance its availability in plants for sustainable agriculture. Vol. 19, International Journal of Molecular Sciences. MDPI AG; 2018.
6. Marschner P. Marschner ' s Mineral Nutrition of Higher Plants. Marschner's Mineral Nutrition of Higher Plants. Orford: Elsevier; 2012. 1–651 p.
7. Yoshinari A, Takano J. Insights into the Mechanisms Underlying Boron Homeostasis in Plants. Front Plant Sci [Internet]. 2017 Nov 17 [cited 2019 Jan 10];8:1951. Available from: http://www.ncbi.nlm.nih.gov/pubmed/29204148.
8. 10.1007/s11104-014-2149-y
   Reid R. Understanding the boron transport network in plants. Plant Soil [Internet]. 2014 Dec 4 [cited 2019 Jan 10];385(1–2):1–13. Available from: http://link.springer.com/10.1007/s11104-014-2149-y.

9. 10.1007/978-1-4419-6315-4_7
Miwa K, Tanaka M, Kamiya T, Fujiwara T. Molecular Mechanisms of Boron Transport in Plants: Involvement of Arabidopsis NIP5;1 and NIP6;1. In Springer, New York, NY; 2010 [cited 2019 Jan 10]. p. 83–96. Available from: http://link.springer.com/10.1007/978-1-4419-6315-4_7.
10. Raven JA. Short- and long-distance transport of boric acid in plants. New Phytol. 1980 Feb;84(2)(1):231–49.
11. Wallace IS, Choi W-G, Roberts DM. The structure, function and regulation of the nodulin 26-like intrinsic protein family of plant aquaglyceroporins. Biochim Biophys Acta (BBA)-Biomembranes. 2006;1758(8):1165–75.
12. http://doi.wiley.com/10.1111/j.1365-3040.2009.02003.x
Fitzpatrick KL, Reid RJ. The involvement of aquaglyceroporins in transport of boron in barley roots. Plant Cell Environ [Internet]. 2009 Oct 1 [cited 2019 Jan 10];32(10):1357–65. Available from: http://doi.wiley.com/10.1111/j.1365-3040.2009.02003.x.
13. Bhattacharjee H, Mukhopadhyay R, Thiyagarajan S, Rosen BP. Aquaglyceroporins: Ancient channels for metalloids. J Biol. 2008;7(9):33.
14. Tanaka M, Wallace IS, Takano J, Roberts DM, Fujiwara T. NIP6;1 Is a Boric Acid Channel for Preferential Transport of Boron to Growing Shoot Tissues in Arabidopsis. Plant Cell. 2008;20(10):2860–75.
15. Takano J, Wada M, Ludewig U, Schaaf G, von Wirén N, Fujiwara T. The Arabidopsis major intrinsic protein NIP5;1 is essential for efficient boron uptake and plant development under boron limitation. Plant Cell [Internet]. 2006 Jun [cited 2017 Dec 7];18(6):1498–509. Available from: http://www.ncbi.nlm.nih.gov/pubmed/16679457.
16. Bienert MD, Bienert GP. Plant Aquaporins and Metalloids. Cham: In Springer; 2017. pp. 297–332.
17. Takano J, Tanaka M, Toyoda A, Miwa K, Kasai K, Fuji K, et al. Polar localization and degradation of Arabidopsis boron transporters through distinct trafficking pathways. Proc Natl Acad Sci U S A. 2010 Mar;107(11):5220–5.
18. Takano J, Noguchi K, Yasumori M, Kobayashi M, Gajdos Z, Miwa K, et al. Arabidopsis boron transporter for xylem loading. Nature. 2002 Nov;420(6913):337–40.
19. Takano J, Miwa K, Fujiwara T. Boron transport mechanisms: collaboration of channels and transporters. Vol. 13, Trends in Plant Science. Elsevier; 2008. p. 451–7.
20. Miwa K, Fujiwara T. Boron transport in plants: co-ordinated regulation of transporters. Ann Bot [Internet]. 2010 Jun [cited 2019 Jan 10];105(7):1103–8. Available from: http://www.ncbi.nlm.nih.gov/pubmed/20228086.
21. Varshney RK, Close TJ, Singh NK, Hoisington DA, Cook DR. Orphan legume crops enter the genomics era! Curr Opin Plant Biol. 2009;12(2):202–10.
22. Brewin NJ. Development of the legume root nodule. Annu Rev Cell Biol. 1991;7:191–226.
23. Patriarca EJ, Tatè R, Iaccarino M. Key Role of Bacterial NH4 + Metabolism in Rhizobium-Plant Symbiosis. Microbiol Mol Biol Rev. 2002 Jun;66(2):203–22.

24. Jones KM, Kobayashi H, Davies BW, Taga ME, Walker GC. How rhizobial symbionts invade plants: The Sinorhizobium - Medicago model. Vol. 5, Nature Reviews Microbiology. NIH Public Access; 2007. p. 619–33.
25. Boyle E. Oceans: Nitrogen pollution knows no bounds. Vol. 356, Science. American Association for the Advancement of Science; 2017. p. 700–1.
26. Kanter DR. Nitrogen pollution: a key building block for addressing climate change. Clim Change. 2018 Mar 1;147(1–2):11–21.
27. 10.1186/s40066-016-0084-2
Dent D, Cocking E. Establishing symbiotic nitrogen fixation in cereals and other non-legume crops: The Greener Nitrogen Revolution [Internet]. Vol. 6, Agriculture and Food Security. BioMed Central Ltd.; 2017 [cited 2020 Jun 5]. p. 7. Available from: http://agricultureandfoodsecurity.biomedcentral.com/articles/10.1186/s40066-016-0084-2.
28. Pankievicz VCS, Irving TB, Maia LGS, Ané JM. Are we there yet? The long walk towards the development of efficient symbiotic associations between nitrogen-fixing bacteria and non-leguminous crops. Vol. 17, BMC Biology. BioMed Central Ltd.; 2019. p. 1–17.
29. White J, Prell J, James EK, Poole P. Nutrient sharing between symbionts. Vol. 144, Plant Physiology. American Society of Plant Biologists; 2007. p. 604–14.
30. Bogacki P, Peck DM, Nair RM, Howie J, Oldach KH. Genetic analysis of tolerance to boron toxicity in the legume Medicago truncatula. BMC Plant Biol. 2013;13(1):54.
31. Takata K, Matsuzaki T, Tajika Y. Aquaporins. Water channel proteins of the cell membrane. Prog Histochem Cytochem. 2004 May;25(1):1–83. 39(.
32. Fageria NK, Baligar C, Clark RB. Micronutrients in crop production. Vol. 77, Advances in Agronomy. Academic Press Inc.; 2002. p. 185–268.
33. Alloway BJ. Micronutrients and crop production: An introduction. Micronutrient Deficiencies in Global Crop Production. Springer Netherlands; 2008. p. 1–39.
34. Hirsch AM, Lum MR, Downie JA. What makes the Rhizobia-legume symbiosis so special? Vol. 127, Plant Physiology. American Society of Plant Biologists; 2001. p. 1484–92.
35. Gupta UC. Boron, molybdenum and selenium status in different plant parts in forage legumes and vegetable crops. J Plant Nutr. 1991;14(6):613–21.
36. 10.1007/BF00012020
Bagheri A, Paull JG, Rathjen AJ, Ali SM, Moody DB. Genetic variation in the response of pea (Pisum sativum L.) to high soil concentrations of boron. Plant Soil [Internet]. 1992 Oct [cited 2020 Jun 5];146(1–2):261–9. Available from: http://link.springer.com/10.1007/BF00012020.
37. Bolaños L, Esteban E, de Lorenzo C, Fernandez-Pascual M, de Felipe MR, Garate A, et al. Essentiality of boron for symbiotic dinitrogen fixation in pea (Pisum sativum) rhizobium nodules. Plant Physiol. 1994;104(1):85–90.
38. Bonilla I, Mergold-Villaseñor C, Campos ME, Sánchez N, Pérez H, López L, Castrejón L, Sánchez F. and GIC. The aberrant cell walls of boron-deficient bean root nodules have no covalently bound

hydroxyproline-/proline-rich proteins. Plant Physiol. 1997;115:1329–40.

39. Bolaños L, Lukaszewski K, Bonilla I, Blevins D. Why. boron? Plant Physiol Biochem PPB / Société Fr Physiol végétale [Internet]. 2004 Dec [cited 2016 Oct 1];42(11):907–12. Available from: http://www.ncbi.nlm.nih.gov/pubmed/15694285.
40. Bolaños L, Brewin NJ, Bonilla I. Effects of boron on Rhizobium-legume cell-surface interactions and nodule development. Plant Physiol. 1996;110(4):1249–56.
41. Mattos D, Hippler FWR, Boaretto RM, Stuchi ES, Quaggio JA. Soil boron fertilization: The role of nutrient sources and rootstocks in citrus production. J Integr Agric. 2017 Jul;16(7)(1):1609–16.
42. Wang Y, Shi L, Cao X, Xu F. Boron Nutrition and Boron Application in Crops. In: Advances in Plant and Animal Boron Nutrition. Springer Netherlands; 2007. p. 93–101.
43. Bienert GP, Chaumont F. Boron and Aquaporins. In: Encyclopedia of Metalloproteins. Springer New York; 2013. p. 291–4.
44. Noguchi K, Yasumori M, Imai T, Naito S, Matsunaga T, Oda H, et al. bor1-1, an Arabidopsis thaliana mutant that requires a high level of boron. Plant Physiol. 1997;115(3):901–6.
45. Miwa K, Fujiwara T. Boron transport in plants: Co-ordinated regulation of transporters. Ann Bot. 2010;105(7):1103–8.
46. Pang Y, Li L, Ren F, Lu P, Wei P, Cai J, et al. Overexpression of the tonoplast aquaporin AtTIP5;1 conferred tolerance to boron toxicity in Arabidopsis. J Genet Genomics. 2010 Jun 1;37(6):389–97.
47. Martinez-Ballesta MDC, Bastías E, Zhu C, Schäffner AR, González-Moro B, González-Murua C, et al. Boric acid and salinity effects on maize roots. Response of aquaporins ZmPIP1 and ZmPIP2, and plasma membrane H+-ATPase, in relation to water and nutrient uptake. Physiol Plant. 2008 Apr;132(4):479–90.
48. Kumar K, Mosa KA, Chhikara S, Musante C, White JC, Dhankher OP. Two rice plasma membrane intrinsic proteins, OsPIP2;4 and OsPIP2;7, are involved in transport and providing tolerance to boron toxicity. Planta. 2014 Jan;239(1):187–98.
49. Cook DR. Medicago truncatula - A model in the making! Vol. 2, Current Opinion in Plant Biology. Current Biology Ltd; 1999. p. 301–4.
50. Tanaka M, Takano J, Chiba Y, Lombardo F, Ogasawara Y, Onouchi H, et al. Boron-Dependent Degradation of *NIP5;1* mRNA for Acclimation to Excess Boron Conditions in *Arabidopsis*. Plant Cell [Internet]. 2011 Sep [cited 2018 Dec 23];23(9):3547–59. Available from: http://www.ncbi.nlm.nih.gov/pubmed/21908722.
51. Kirscht A, Kaptan SS, Bienert GP, Chaumont F, Nissen P, de Groot BL, et al. Crystal Structure of an Ammonia-Permeable Aquaporin. PLoS Biol. 2016 Mar 30;14(3).
52. Murata K, Mitsuoka K, Hiral T, Walz T, Agre P, Heymann JB, et al. Structural determinants of water permeation through aquaporin-1. Nature. 2000 Oct 5;407(6804):599–605.
53. Redondo-Nieto M, Pulido L, Reguera M, Bonilla I, Bolaños L. Developmentally regulated membrane glycoproteins sharing antigenicity with rhamnogalacturonan II are not detected in nodulated boron

deficient Pisum sativum. Plant, Cell Environ. 2007;30(11).

54. Reguera M, Abreu I, Brewin NJ, Bonilla I, Bolaños L. Borate promotes the formation of a complex between legume AGP-extensin and Rhamnogalacturonan II and enhances production of Rhizobium capsular polysaccharide during infection thread development in Pisum sativum symbiotic root nodules. Plant, Cell Environ. 2010;33(12).
55. Reguera M, Wimmer M, Bustos P, Goldbach HE, Bolaños L, Bonilla I. Ligands of boron in Pisum sativum nodules are involved in regulation of oxygen concentration and rhizobial infection. Plant, Cell Environ. 2010;33(6).
56. Reguera M, Espí A, Bolaños L, Bonilla I, Redondo-Nieto M. Endoreduplication before cell differentiation fails in boron-deficient legume nodules. Is boron involved in signalling during cell cycle regulation?: Letter. New Phytol. 2009;183(1).
57. Brito B, Palacios JM, Hidalgo E, Imperial J, Ruiz-Argueso T. Nickel availability to pea (Pisum sativum L.) plants limits hydrogenase activity of Rhizobium leguminosarum bv. viciae bacteroids by affecting the processing of the hydrogenase structural subunits. J Bacteriol. 1994;176(17):5297–303.
58. Kato Y, Miwa K, Takano J, Wada M, Fujiwara T. Highly boron deficiency-tolerant plants generated by enhanced expression of NIP5;1, a boric acid channel. Plant Cell Physiol. 2009;50(1):58–66.
59. Murashige T, Skoog F. A Revised Medium for Rapid Growth and Bio Assays with Tobacco Tissue Cultures. Physiol Plant. 1962 Jul;15(3):473–97.
60. Kazmierczak T, Nagymihaly M, Lamouche F, Barriére Q, Guefrachi I, Alunni B, et al. Specific host-responsive associations between medicago truncatula accessions and sinorhizobium strains. Mol Plant-Microbe Interact. 2017;30(5):399–409.
61. Hardy RWF, Holsten RD, Jackson EK, Burns RC. The acetylene - ethylene assay for N2 Fixation: laboratory and field evaluation. Plant Physiol. 1968;43:1185–207.
62. 10.1186/1746-4811-4-18
Kakar K, Wandrey M, Czechowski T, Gaertner T, Scheible WR, Stitt M, et al. A community resource for high-throughput quantitative RT-PCR analysis of transcription factor gene expression in Medicago truncatula. Plant Methods [Internet]. 2008 Jul 8 [cited 2020 Jun 5];4(1):18. Available from: http://plantmethods.biomedcentral.com/articles/10.1186/1746-4811-4-18.
63. Boisson-Dernier A, Chabaud M, Garcia F, Bécard G, Rosenberg C, Barker DG. Agrobacterium rhizogenes-transformed roots of Medicago truncatula for the study of nitrogen-fixing and endomycorrhizal symbiotic associations. Mol Plant-Microbe Interact. 2001;14(6):695–700.
64. Vincent JM. A manual for the practical study of the root-nodule bacteria. A manual for the practical study of the root-nodule bacteria. London: IBP Handbk 15 Oxford and Edinburgh: Blackwell Scientific Publications; 1970. 164 p.
65. Nakagawa T, Ishiguro S, Kimura T. Gateway vectors for plant transformation. Plant Biotechnol. 2009;26(3):275–84.
66. Vernoud V, Journet EP, Barker DG. MtENOD20, a nod factor-inducible molecular marker for root cortical cell activation. Mol Plant-Microbe Interact. 1999 Feb;19(7):604–14. 12(.

67. Ashby AM, Watson MD, Loake GJ, Shaw CH. Ti plasmid-specified chemotaxis of Agrobacterium tumefaciens C58C1 toward vir-inducing phenolic compounds and soluble factors from monocotyledonous and dicotyledonous plants. J Bacteriol. 1988;170(9):4181–7.
68. Yang K, Rong W, Qi L, Li J, Wei X, Zhang Z. Isolation and characterization of a novel wheat cysteine-rich receptor-like kinase gene induced by Rhizoctonia cerealis. Sci Rep. 2013 Oct;23(1):1–10. 3(.
69. Voinnet O, Rivas S, Mestre P, Baulcombe D. An enhanced transient expression system in plants based on suppression of gene silencing by the p19 protein of tomato bushy stunt virus. Plant J. 2003 Mar;33(5):949–56.
70. Sparkes IA, Runions J, Kearns A, Hawes C. Rapid, transient expression of fluorescent fusion proteins in tobacco plants and generation of stably transformed plants. Nat Protoc. 2006;1(4):2019–25.
71. Zhang X, Henriques R, Lin SS, Niu QW, Chua NH. Agrobacterium-mediated transformation of Arabidopsis thaliana using the floral dip method. Nat Protoc. 2006 Jul;1(2):641–6.

Figures

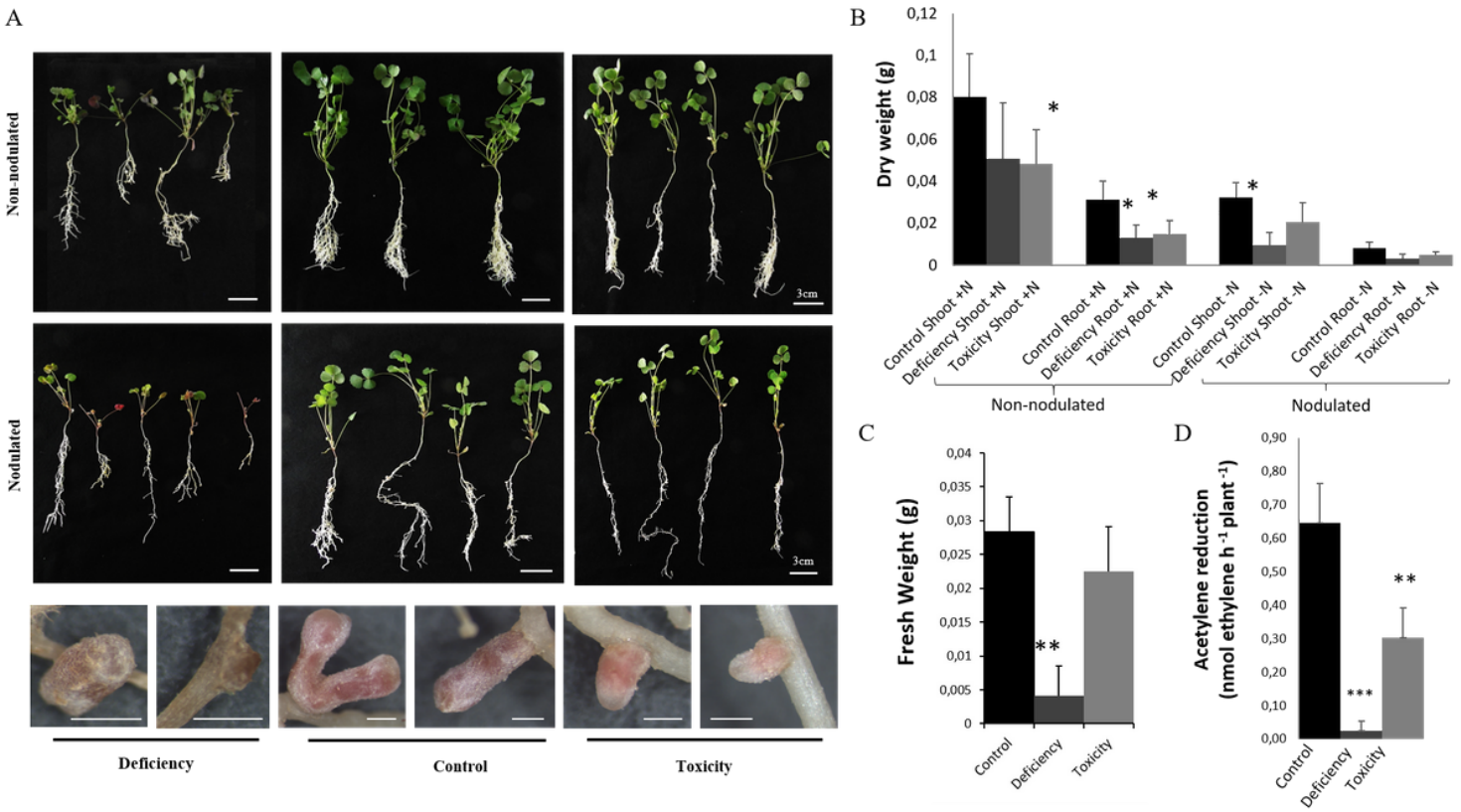

Figure 1

Boron stress has an inhibitory effect on M. truncatula growth and on the nitrogenase activity. A) Pictures of 4-week-old M. truncatula plants growing under a B gradient are shown. Upper panels (upper row of images) show plants fertilized with N (non-nodulated plants) growing under B deficiency (no B was

supplemented into the media), control (media at a final B concentration of 0,1mM B[OH3]) or B toxic conditions (1mM B[OH3]). Middle row of images shows plants growing under symbiotic conditions (M. truncatula plants inoculated with S. meliloti 2011). Lower row of images shows nodules from plants grown under different B conditions, as indicated in the bottom labels. Bar=3cm (plant pictures) or 1mm (nodule pictures). B) Plant biomass as dry weight of roots and shoots of non nodulated or nodulated plants under a B gradient C) Nodule fresh weight under a B gradient. Data are the Mean ± SD of two independent experiments with, at least, four biological replicates (n=4). D) Nitrogenase activity was determined in 4-week-old plants growing under a B gradient. Plants growing under control, B deficiency or B toxic conditions were used to evaluate nitrogenase activity changes under different B conditions. Nitrogenase activity was analyzed by the acetylene reduction method (nmol ethylene generated per hour per plant). Data were analyzed using One-way analysis of variance (ANOVA) followed by t-student post-hoc test. Asterisks indicate significant differences when comparing B stress samples with B control treatment (t-Student, (“*”= p<0.05, “**” = p<0.01, , “***” = p<0.001).

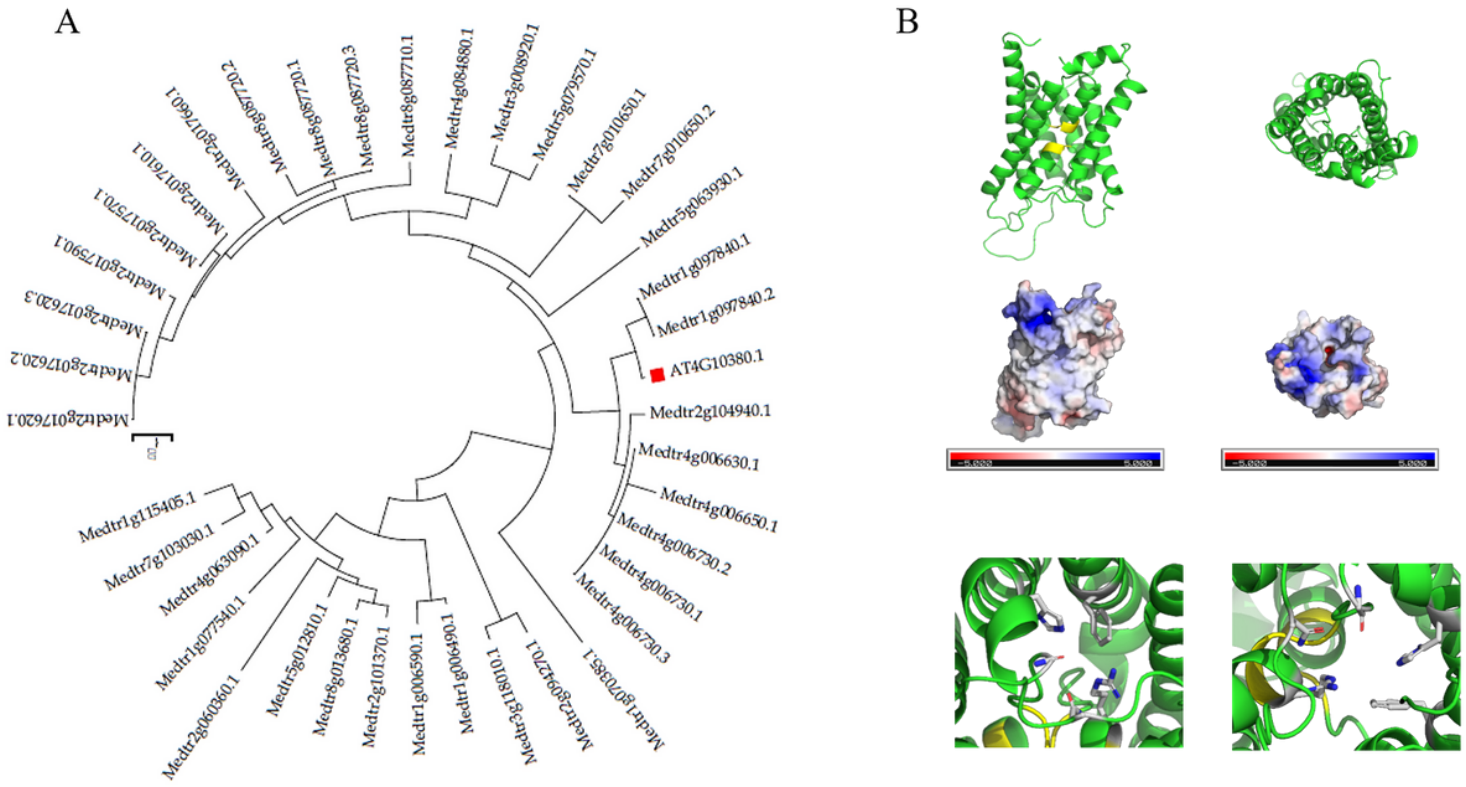

Figure 2

M. truncatula MtNIP5;1 is the closest homologous protein to the A. thaliana AtNIP5;1, an aquaporin involved in B transport under deficiency. (A) Unrooted phylogenetic tree of M. truncatula homologues to AtNIP5;1 (which is indicated by a red square) was obtained using Mega7 software. The tree is drawn so that branch length separating any two sequences is proportional to evolutionary distances (B) MtNIP5;1 protein predicted model. Upper panel within panel B indicates the tertiary structure model of MtNIP5;1 showing yellow areas that represent the NPA motifs. Distribution of positive (blue) and negative (red) charges are shown below. The location of positive charged residues in the external part of the pore

leaving the negative charges in the inside are shown. The bottom part of panel B shows the five amino acids (F58, N129, H180, G190 and R197) that would conform the selectivity filter of MtNIP5;1.

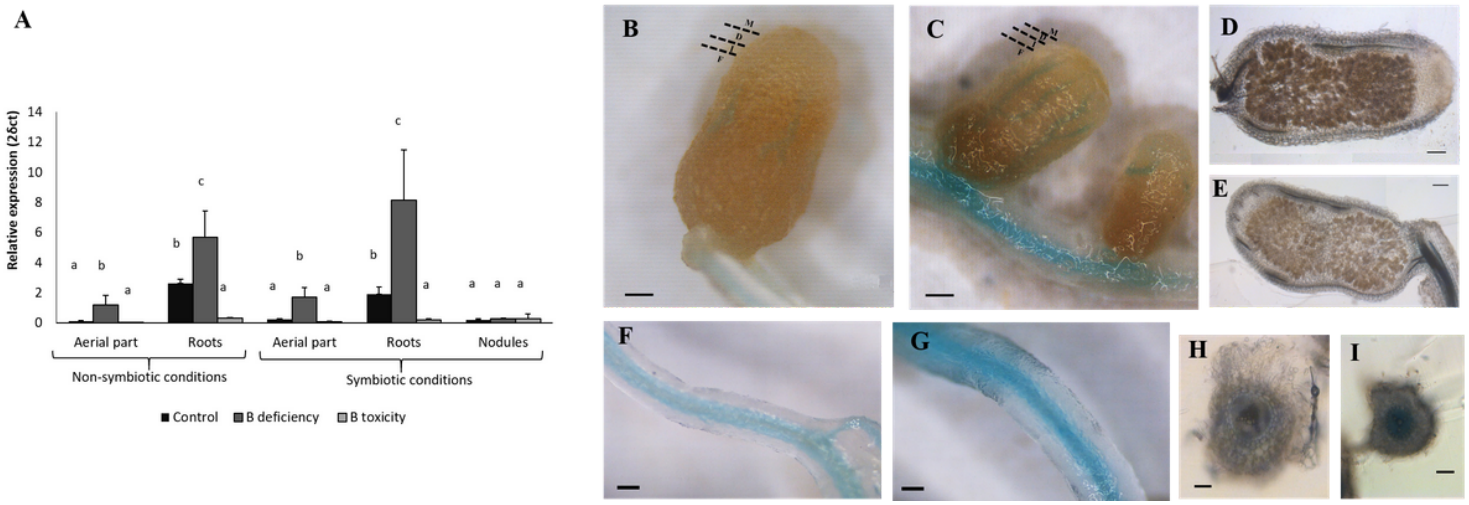

Figure 3

MtNIP5;1 expression is induced under B deficiency A) mRNA accumulation was quantified by qPCR in roots, shoots and nodules of plants fertilized with N or growing under symbiotic conditions. Plants grew under a B gradient consisting of the following treatments: control conditions (0,1mM B[OH3]), deficiency (0mM B[OH3]), or B toxicity (1mM B[OH3]). Data are the Mean ± SD of two independent experiments with, at least, four pooled plants and four biological replicates (n=4). Different letters indicate significant differences (One-way ANOVA followed by Tukey test, $p<0.05$). MtNIP5;1 expression is presented as expression relative values to the internal gene Ubiquitin carboxyl-terminal hydrolase 1. B-I) Tissue expression localization of pMtNIP5;1 ::GUS appears at the vasculature and is induced under B deficiency. Blue GUS staining analysis in pMtNIP5;1::GUS appears in the vasculature of B-E: nodules and F-I: roots. B, D, F and H show B control treatment (0,1mM B[OH3]), C, E, G and I: B deficiency treatment. M: meristematic zone, D: differentiation zone, I: interzone F: N2 fixation zone. Bar=0,5cm.

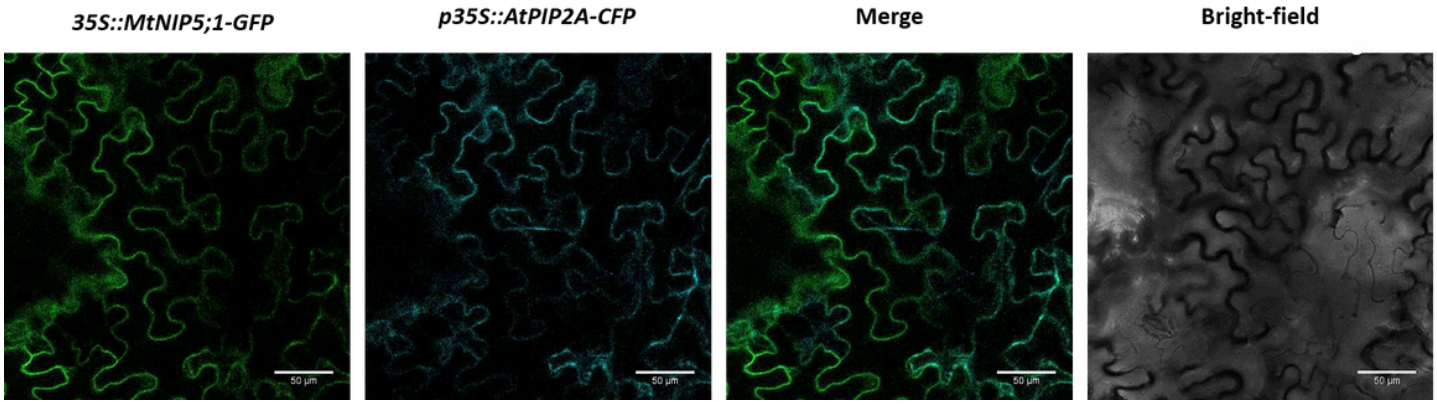

Figure 4

Subcellular localization of MtNIP5;1 in N. benthamiana leaves evidences its localization at the plasma membrane. Left panel shows the GFP signal of MtNIP5;1-GFP, left middle panel shows CFP signal of

AtPIP2A-m-cherry, right middle panel shows GFP and CFP merged images and right panel the bright field image. p35S::MtNIP5;1-GFP and p35S::AtPIP2A- cyan fluorescent protein (CFP) were co-transformed into N. benthamiana leaves. Bar=50µm.

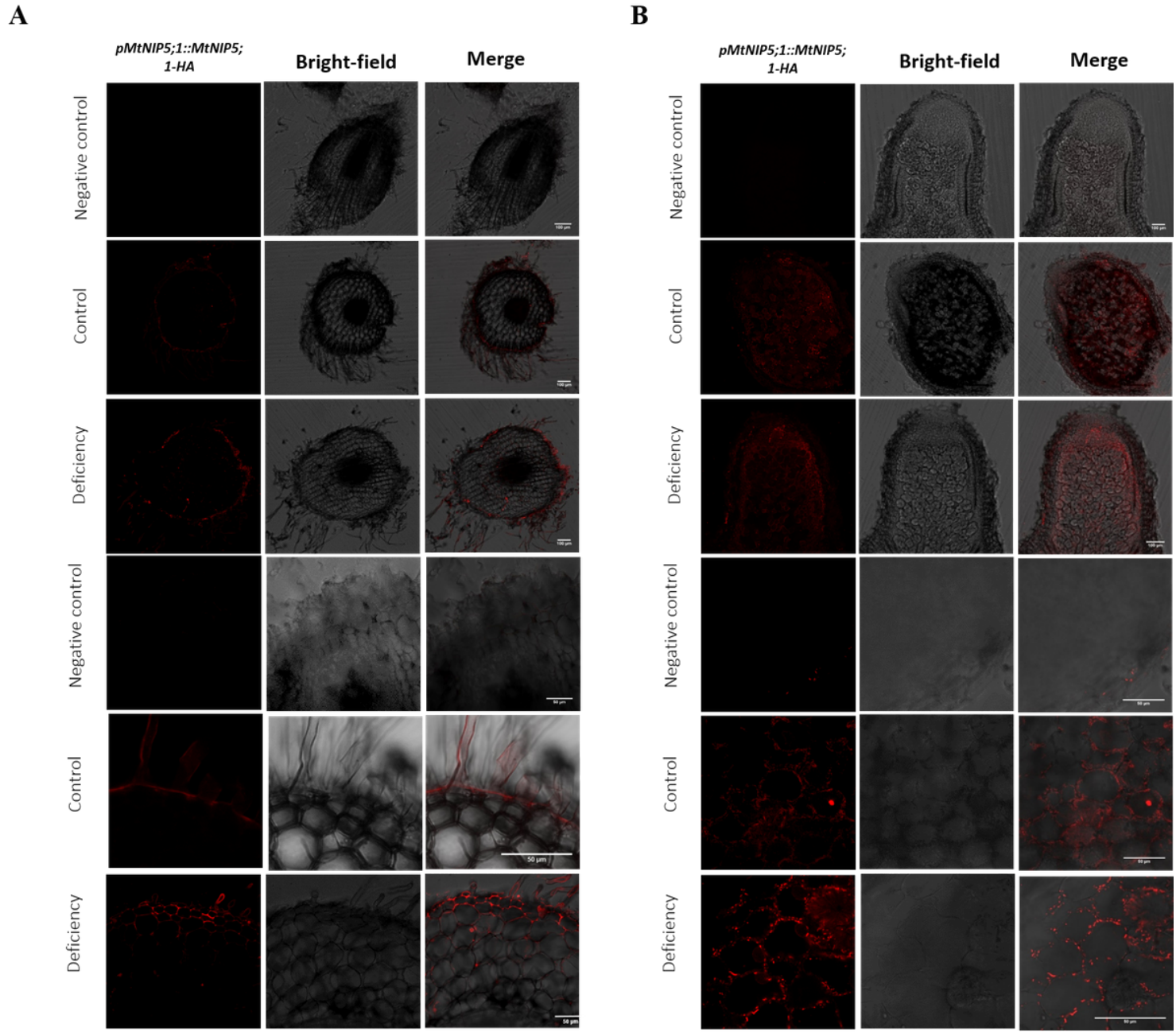

Figure 5

Inmunolocation of MtNIP5;1 in the root epidermis and nodules of Medicago truncatula A) Subcellular localization by immunostaining of MtNIP5;1-HA with the antibody Alexa 594 was performed in root sections of 4-week-old M. truncatula expressing p35S::MtNIP5;1-HA (red, , DsRed channel) under different B conditions (control and deficiency). The three bottom rows show detail of root epidermal and hair root cells showing MtNIP5;1-HA localization. B) Subcellular localization by immunostaining of MtNIP5;1-HA with the antibody Alexa 594 was performed in nodule sections of 4-week-old M. truncatula expressing

p35S::MtNIP5;1-HA (red, DsRed channel), inoculated with a Sinorhizobium meliloti 2011 strain and growing under different B conditions (control, middle row, and deficiency, bottom row). The three bottom rows show detail of nodule cortex and fixation zone showing MtNIP5;1-HA localization. Left column images show HA signal, middle column shows bright field images and right column shows the merged images of HA signal and bright field. Upper rows in each panel show autofluorescence controls, in which no anti-HA primary antibody was used. Bars=100µm or 50µm.

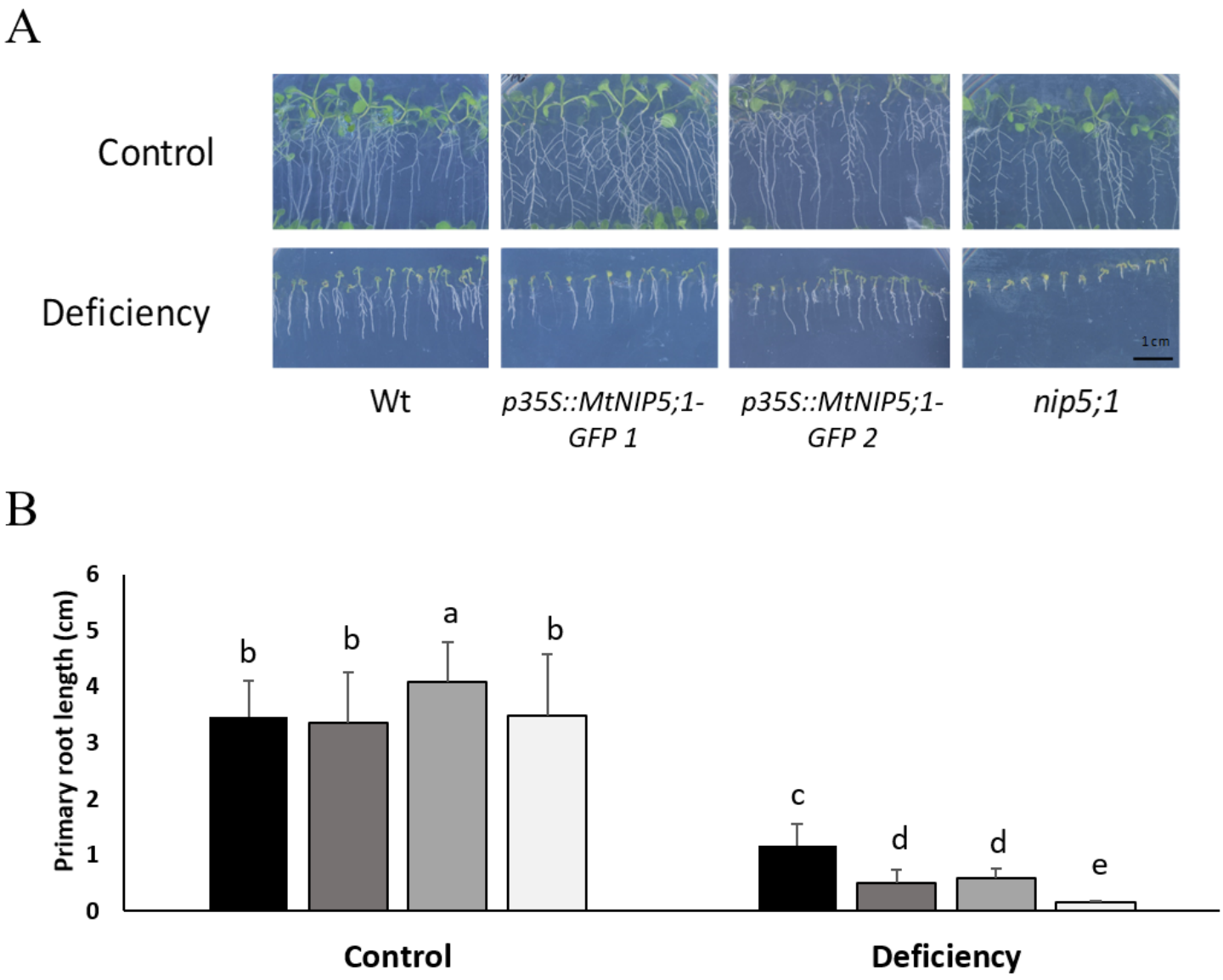

Figure 6

MtNIP5;1 partially complements nip5;1 B deficiency phenotype. Primary root growth of A. thaliana seedlings in nip5;1 complementation assays are presented. A) Images of seedlings (Wild type (Wt), p35S::MtNIP5;1-GFP 1, p35S::MtNIP5;1-GFP 2 and nip5;1) growing under control (upper row) or B deficient conditions (bottom row). B) Primary root growth of Wt (black column), two independent lines expressing p35S::MtNIP5;1-GFP (p35S::MtNIP5;1-GFP 1 and p35S::MtNIP5;1-GFP 2, dark and light grey columns, respectively), and nip5;1 (white column) was measured 10 days postgermination (X axis).

Seedlings were grown under two B treatments: control (100µM B[OH3]) and deficiency (0,03µM B[OH3]). Different letters indicate significant differences using a One-way ANOVA analysis followed by Tukey's test ($p<0.05$).

Supplementary Files

This is a list of supplementary files associated with this preprint. Click to download.

- AdditionalFile7.pdf
- AdditionalFile6.pdf
- AdditionalFile5.pdf
- AdditionalFile4.pdf
- AdditionalFile3.pdf
- AdditionalFile2.pdf
- AdditionalFile1.pdf